Aerospace Science and Technology 45 (2015) 150–153

Contents lists available at ScienceDirect

Aerospace Science and Technology

www.elsevier.com/locate/aescte

Short communication

Universal erosive burning model performance for solid rocket motor internal ballistics

Afroz Javed, Debasis Chakraborty *

Directorate of Computational Dynamics, Defence Research and Development Laboratory, Hyderabad 500058, India

ARTICLE INFO

Article history:
Received 3 March 2015
Received in revised form 6 May 2015
Accepted 14 May 2015
Available online 15 May 2015

Keywords:
Erosive burning
Finocyl grain
Solid rocket motor

ABSTRACT

The erosive burning of solid rocket propellant is an area of concern for high L/D rocket motors. Several explanations for the different causes for this phenomenon exist along with the modelling practices to predict the effects based on these causes. Universal nature of the erosive burning process was proposed by Mukunda and Paul irrespective of size, shape and type of the propellant. In the present work, the same model is applied for cylindrical port motors with high and moderate mass flux, as well as finocyl grain motors. It is observed that for cylindrical port motors, computed pressures with the burning time match very well experimental data. A modified form of the model (which becomes the original model for axisymmetric port) is used for finocyl geometries and a good prediction of pressures is observed. This study confirms the universality of the Mukunda and Paul model in its modified form which addresses non-axisymmetric port geometries also. The simplicity of the model makes it a useful tool for design and analysis of solid rocket motors of any size and port geometry.

1. Introduction

The augmentation of the normal burning rate of a solid propellant due to the presence of high velocity gases flowing parallel to the burning surface is referred to as erosive burning. In ported solid rocket motors, the flow velocity parallel to the burning surfaces is lowest near the head end, as the flow proceeds downstream the velocity goes on increasing due to mass addition from the combustion of the propellant. This makes likelihood of erosive burning to occur at the aft end of the propellant grain where the core flow is greatest. The speed of the flow has a large impact on the amount of erosive burning that might occur. As the gas velocity increases, so does erosive burning. Hence, port geometries that generate high speed gas flow at the aft end of the motor also increase the possibility of erosive burning. The gas velocity is mainly controlled by two parameters which are the length of the port compared to its diameter (L/D ratio) and the area ratio of the port compared to that of the throat (port/throat area ratio). The total impulse deliverable by a solid rocket motor is directly proportional to the amount of propellant in the motor, increasing the overall length or decreasing the port diameter would result in increased total impulse. But this would also increase the L/D of the motor. The performance of a motor can also be improved by increasing the chamber pressure. This can be achieved by decreasing the throat area for the same propellant composition, which in turn increases port/throat area ratio. Both of these changes result in an increase in core flow speed. In order to increase the propellant loading and decrease the chances of erosive burning, many large solid rocket motors are designed with ports that increase in size towards the aft end. With the need for higher propellant loadings in rocket motors, and consequent use of low port-to-length-ratio channels and of narrow-slotted grains (finocyl), high specific mass flow rates and velocities are observed at the aft end. There are also rocket motor designs using nozzleless configuration in which the flow velocity becomes sonic within the propellant grain. These make the understanding and the prediction of erosive burning a matter of important concern.

Several studies were carried out in the past to understand and model the erosive burning phenomenon. In general, there is an agreement that the augmentation of the burning rate due to the flow velocities is caused by enhanced heat transfer to the propellant surface when compared with the case of nearly zero flow velocities of the products of combustion over the burning surface. Lenoir and Robillard [1] provided the first comprehensive analysis based on this mechanism assuming flat-plate type scaling of the heat transfer. Other authors have considered compressibility effects [2] and turbulence effects [3] in semi-empirical treatments. More recently, time-accurate computational-fluid-dynamics simulations [4,5] attribute heat-transfer enhancement to penetration of turbulent eddies into the near-propellant region. Godon et al. [6] studied the erosive burning of ammonium perchlorate inert

* Corresponding author.
E-mail address: debasis_cfd@drdl.drdo.in (D. Chakraborty).

http://dx.doi.org/10.1016/j.ast.2015.05.005
1270-9638/

binder propellants both experimentally and from modelling viewpoint. A correlation law was obtained for shear stress. King [7] has discussed general modelling practices and models suggested by different researchers. These models utilise either and/or a combination of the phenomena of heat transfer, flame bending, turbulence interaction, chemically reacting boundary layer theory etc. to predict the erosive burn rate. Mukunda and Paul [8] found out a relatively simple nondimensional relationship between the ratio of the actual to nonerosive burn rate that matched well with the experiments. It was concluded that the correlation may be adopted universally for most practical propellants. Mukunda et al. [9] have further presented a correction in their original model to address partly symmetric grain geometries. In the present work Mukunda and Paul [8] model is applied for the prediction of erosive burning in cylindrical motor geometries from Hasegawa et al. [10] experimental cases, and its modified form [9] for finocyl grain motors.

2. Mukunda and Paul erosive burning model [8]

Extensive data and correlations on the erosive burning of solid propellants are considered for the development of this model. The erosive burning data of a range of propellants from double-base to composite, varying energy levels, and different base burn rates are analysed and these data show a universality in the relationship between the erosive burning rate ratio and a nondimensional mass flux and the Reynolds number, based on the nonerosive burn rate and port diameter, with the underlying assumption that the phenomenon is fluid dynamically controlled. An examination of the data shows that such a hypothesis is indeed valid to within the experimental accuracies in the measurement. The chemical kinetic factors, if any, have such a minor role that they do not make any distinct contribution to the effects of erosive burning beyond experimental noise. The data are curve-fitted into an expression which can be used for most practical propellants to within ±10% accuracy.

The modified burn rate is given as,

$$\dot{r}_{erosive} = \dot{r}\left(1 + 0.023\left(g^{0.8} - g_{th}^{0.8}\right)\mathcal{H}(g - g_{th})\right) \quad (1)$$

Here g is essentially the ratio of mass flux through the port to the mass efflux from the surface modified for size effects as $(G/\rho_p\dot{r})(\rho_p\dot{r}d_0/\mu)^{-0.125}$, with G the mass flux through the port, $\rho_p\dot{r}$ is the non-erosive mass efflux from the surface, g_{th} is the threshold value obtained from the plot of the data as 35 and $\mathcal{H}$ is the Heaviside step function that is introduced to indicate a critical flux below which there is no erosive burning. The dynamic viscosity of the combustion gases is represented by μ. The value of d_0 is taken as diameter for cylindrical port motors, for non-cylindrical geometries use of hydraulic diameter $(4A/P)$ is suggested, P is the perimeter of the grain port and A is cross sectional area. When this relationship was used for grain shapes having finocyl geometries [11], the pressure variation with time was overpredicted. To address this anomaly, modification was proposed by Mukunda et al. [9] after analysing the flow field in finocyl grain motors as discussed in the next section.

3. Modified Mukunda and Paul model [9]

The original Mukunda and Paul [8] model when applied to axisymmetric port geometries gives satisfactory results. However when applied to grains with partly symmetric geometries like finocyl [11], it tends to predict higher pressures than experimentally observed in the early part of burning. This issue was addressed by Mukunda et al. [9] by analysing the flow field inside finocyl rocket motors using CFD techniques. It was observed that the dimensionless wall shear remains nearly the same on different axial locations of the slotted part of the motor. Also it is observed that the wall shear is less in the recess region. The shear stress directly controls the heat transfer to the surface and hence the local burn rate along the surface. This azimuthal variation of burn rate is also observed experimentally by Dickinson et al. [12] using an arm grain configuration. The CFD studies made it clear that the motor sizing parameter should address the equivalent average shear stress. The use of hydraulic diameter ensures same pressure drops in flows in tubes, however, to ensure same shear stress on the surface the equivalent diameter is found to be P/π where P is the perimeter of the grain port. With this modification it was shown that the initial overprediction of pressure was no more observed for finocyl grain motors.

Table 1
Geometrical properties of cylindrical motors.

	Type A	Type B	Type C
Nozzle throat diameter (mm)	34	23	34
Initial port diameter (mm)	40	40	60
Grain length (mm)	1680	840	1260

4. Cylindrical motors

Experimental studies on cylindrical motors by Hasegawa et al. [10] are considered for the validation of Mukunda and Paul [8] universal erosive burning model. It is important to note that the experimental investigations of Hasegawa et al. [10] are reported in 2006 whereas Mukunda and Paul [8] original erosive burning model was proposed in 1997 and hence it is a good case for validation of the model. The cylindrical motors studied by Hasegawa et al. [10] were cast using a composite propellant with the composition of 69% AP, 17% HTPB, and 14% aluminium. The density of the propellant was 1700 kg/m^3, linear burning rate was 4.9 mm/s at 49 bar pressure and 20 °C temperature, pressure exponent value was 0.3, the adiabatic flame temperature was reported to be 3041 K at 50 bar with frozen flow, mean molecular mass as 25.4 g/mol, and ratio of specific heats was 1.19. The viscosity of the products of combustion using NASA CEA600 [13] comes out to be 9.016×10^{-5} Pa s. Three different motors namely type A, B, and C with outer shell diameters of 80 mm were tested with this propellant. The geometrical properties of these motors are given in Table 1.

Hasegawa et al. [10] have used a simplified erosive burning law suggested by Dickinson et al. [12] to predict the erosive burning phenomena. The coefficients of this model are evaluated through the experimental studies of Double Slab Motors (DSM). It was found that the correlation was satisfactory for the similar mass flux as used in DSM but for higher mass flux it required modifications.

The p–t curve of type 'A' motor evaluated using Mukunda and Paul [8] erosive burning model is shown in Fig. 1(a). The experimental curve is also shown for comparison. It can be seen that the pressures in the initial burn time and location of pressure peak show very good match with the experimental result. The original model of Hasegawa et al. [10] shows lower values of pressures throughout the burn time. This behaviour is attributed to higher mass flux as compared with DSM motors. Modifications in the model parameters are made and modified Hasegawa et al. [10] model could capture the experimental p–t curve. While Hasegawa model needed corrections for high mass flux and type of propellant, fairly accurate pressures could be predicted using Mukunda and Paul [8] model in its original form without requiring any modification to handle high mass flux.

Fig. 1(b) depicts the p–t curve for type 'B' motor. A good match of pressures is found initially for type 'B' motor, while after around 2.0 s the predicted pressures show values higher than

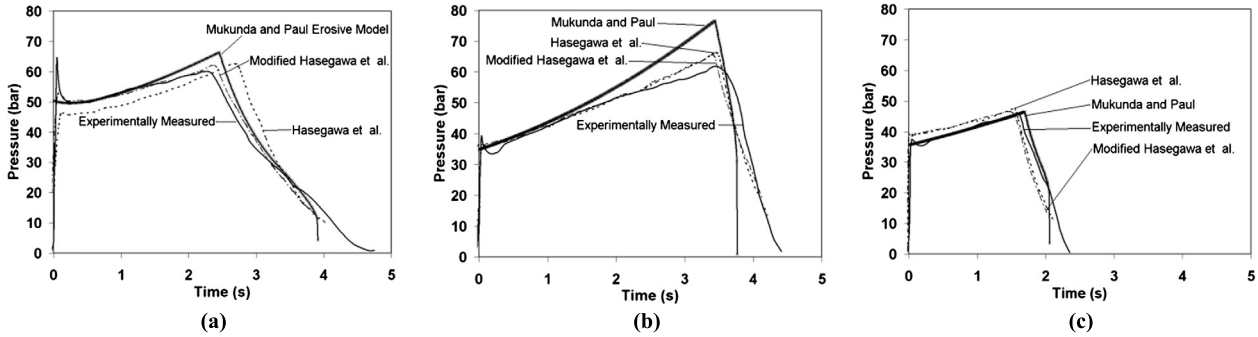

Fig. 1. The experimental p–t curves of (a) type 'A' motor, (b) type 'B' motor and (c) type 'C' motor with predictions using different erosive burning models.

that observed experimentally as well as predicted by Hasegawa et al. The maximum difference in the pressures predicted using Mukunda and Paul [8] model is around 18% when compared with the experimental values and 12% higher than those predicted using Hasegawa et al. [10] models. The change of throat diameter during the firing may be an explanation for the higher pressures predicted for type 'B' motor near the latter part of the burn time. Also it is to be noted that although the mass flux through the throats of both the type 'A' and type 'B' motors are nearly equal, the throat diameter of type 'B' motor is around 32% smaller than that of type 'A' as can be seen in Table 1. This smaller perimeter may be a cause for higher heat transfer loads and consequent throat erosion. The internal ballistic program used for the predictions in the present case does not consider the change in throat diameter due to erosion or adhesion of Al/Al_2O_3, while the prediction program used by Hasegawa et al. [10] takes into consideration the change of throat diameter as linear with time. However the exact throat diameters changes considered are not discussed by Hasegawa et al. [10] With this consideration of throat diameter change a good match of predicted pressures from both original and modified Hasegawa et al. [10] erosive burning models is found with the experimental pressure. For the type 'B' motor with lower port mass flux values both the original and modified Hasegawa et al. [10] models predict nearly the same p–t curve. Notwithstanding the differences observed in the predicted and experimental p–t curves in the later part of the burning, all the three models considered show a good match in the beginning of burn time with the presence of erosive burning effects.

The comparisons of predicted and experimental p–t curves for type 'C' motor are shown in Fig. 1(c). Good match of the predicted pressures are obtained for type 'C' motor with the experimental results. The type 'C' motor has a lower burn time as well as lower throat mass flux reducing the occurrence of significant and noticeable throat erosion. This absence of throat erosion manifests itself in a very good match of predicted and experimental pressures from Mukunda and Paul [8] model. The predicted pressures using Hasegawa et al. [8] models are on a slightly higher side by around 5% when compared with experimental pressure history.

5. Motors with finocyl geometries

As discussed earlier the original Mukunda and Paul [8] erosive burning model fails to predict the pressures satisfactorily in non-axisymmetric port geometries. The modified form of Mukunda–Paul [9] model is shown to predict the pressures in non-axisymmetric geometries also. It is to be noted that the modified model [9] degenerates to original model [8] for cylindrical port geometries. In the present study two motors with finocyl geometry are considered for the validation purpose. Both these motors have finocyl geometries with four fins. The salient features of these motors are shown in Table 2.

Table 2
Salient features of the motors considered for internal ballistic analysis.

Motor	Motor-1	Motor-2
Grain length (m)	3.8	1.727
Grain diameter (m)	0.41	0.17
Throat diameter (mm)	116	40
Burn rate at 7 MPa (mm/s)	9.6	8.2
Pressure index	0.44	0.30
Maximum pressure (bar)	104	124
Parameters obtained using NASA CEA 600 [13]		
Adiabatic flame temperature (K)	3386	2750
Molecular weight	19.2	24.8
Ratio of specific heats	1.266	1.19
Dynamic viscosity μ (Pa s)	8.85×10^{-5}	9.34×10^{-5}

The pressures are normalised by the maximum pressures occurring for the particular cases. These maximum pressures used for the purpose of normalisation are also shown in Table 2. The variations of the normalised head end pressure with time are plotted in Figs. 2 and 3.

The Motor-1 p–t curve is shown in Fig. 2. The predicted pressure is initially around 3% higher than the experimental pressure values but this difference goes on reducing with burn time. A zoomed view of the p–t curve near the initial burn time is shown at the inset of the same figure. It is observed that the pressures predicted using original Mukunda–Paul [8] model are around 3% higher than those predicted using the modified version [9] of the model. The modified version predicts the pressures nearer to the experimental pressures. The p–t curve for Motor-2 is shown in Fig. 3. A slightly lower (5%) value of the head end pressures are observed initially from the predicted results when compared with the experimental head end pressures. The time instant ($\approx$0.5 s) of occurrence of pressure peaks for both the experimental and predicted results match well with each other. After the initial stage ($\approx$1.0 s) the difference goes on decreasing and both the experimental and predicted pressures match well till around 5 s of burn time. Near the end of the burning the predicted pressure shows a higher and slightly earlier pressure peak than that observed experimentally. This difference could be present due to the throat erosion and associated decrease in chamber pressure. A zoomed view of the p–t curve near the initial burn time is also shown in the same figure. It is observed that during the first 0.4 s of burning, the pressures predicted using original model [8] show overall less difference with the experimental pressures. A closer examination reveals that the predicted values form a shallow curve which does not conform to the shape of the experimental curve, whereas the modified Mukunda–Paul [9] erosive burning model despite predicting a lower pressure ($\approx$5% lesser than the original model) shows a nearly parallel curve to the experimental pressure values. Since the difference is small and the experimental data is having some error band, no efforts are undertaken to resolve the difference further.

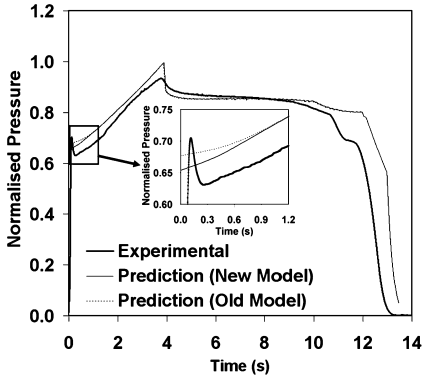

Fig. 2. Experimental p–t curve for Motor-1 with old and new Mukunda–Paul erosive burning model.

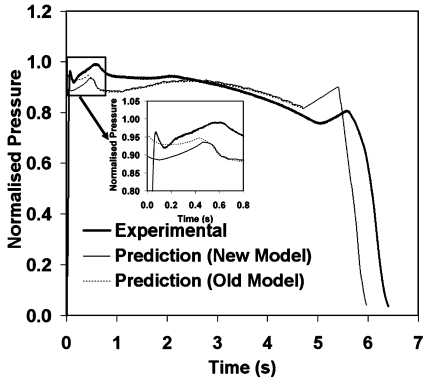

Fig. 3. Experimental p–t curve for Motor-2 with old and new Mukunda–Paul erosive burning model.

It is observed that the modified Mukunda–Paul [9] model is able of predicting the erosive burning in rocket motors with finocyl grain geometry by employing a small modification in the representative diameter scaling. Although the azimuthal burn rate may not be same in non-axisymmetric cross sections under erosive burning conditions as observed by Dickinson et al. [12], the averaged effect of the erosive burning is well captured by the modified Mukunda–Paul [9] model.

6. Conclusions

The internal ballistics calculations of three cylindrical port solid rocket motors are performed using Mukunda–Paul [8] universal erosive burning law. A good match of the pressure history is found in contrast to the Hasegawa et al. [10] model which needed to be modified to accommodate higher mass flux case. Further application of this model on finocyl grain motors has shown overprediction of pressures in the initial burn time which is corrected by using modified Mukunda–Paul model [9]. This study confirms the universality of the Mukunda–Paul [9] model in its modified form which addresses non-axisymmetric port geometries also. Although the exact variations of the burn rate in azimuthal direction are not addressed, the average burn rate increase and its effect due to erosive burning are satisfactorily captured. The simplicity of the model makes it a useful tool for design and analysis of solid rocket motors of any size and port geometry.

Conflict of interest statement

There are no conflicts of interests.

Acknowledgements

The authors are thankful to Mr. Sampath Kumar, Sc. 'F', and Dr. K.K. Rajesh, Sc. 'E', from DOP, DRDL, Mr. M. Rathnam Sc. 'E' and Mr. Guru Sudhakar, Sc. 'C', from SPSC, ASL for providing the motor geometries and test data. The authors also acknowledge the help of Dr. Iyer Arvind Sundaram for development of an internal ballistic code which could be used for complex finocyl geometries incorporating the erosive burning models.

References

[1] J.M. Lenoir, G. Robillard, A mathematical method to predict the effects of erosive burning in solid propellant rockets, in: Proceedings of the 6th Symposium (International) on Combustion, Reinhold Publishing Corporation, New York, 1957, pp. 663–667.
[2] L. Green, Erosive burning of some composite solid propellants, Jet Propuls. 24 (9) (1954) 8–15.
[3] M.K. Razdan, K.K. Kuo, Erosive burning study of composite solid propellants by turbulent boundary-layer approach, J. Propuls. Power 17 (11) (Nov. 1979) 1225–1233.
[4] B.A. McDonald, S. Menon, Direct numerical simulation of solid propellant combustion in crossflow, J. Propuls. Power 21 (3) (2005) 460–469.
[5] T.L. Jackson, Modeling of heterogeneous propellant combustion: a survey, AIAA J. 50 (5) (2012) 993–1006.
[6] J.C. Godon, J. Duterque, G. Lengelle, Erosive burning in solid propellant motors, J. Propuls. Power 9 (6) (1993) 806–811.
[7] M.K. King, Erosive burning of solid propellants, J. Propuls. Power 9 (6) (1993) 785–805.
[8] H.S. Mukunda, P.J. Paul, Universal behavior in erosive burning of solid propellants, Combust. Flame 109 (1–2) (1997) 224–236.
[9] H.S. Mukunda, P.J. Paul, Afroz Javed, Debasis Chakraborty, Extension of the universal erosive burning law to partly symmetric propellant grain geometries, Acta Astronaut. 93 (2014) 176–181.
[10] H. Hasegawa, M. Hanzawa, S. Tokudome, M. Kohno, Erosive burning of aluminized composite propellants: X-ray absorption measurement, correlation, and application, J. Propuls. Power 22 (5) (2006) 975–983.
[11] F. Serraglia, B. Favini, M. di Giacinto, A. Neri, Gasdynamic features in solid rocket motors with finocyl grain during ignition transient, in: Proceedings of the Fifth European Symposium on Aerothermodynamics for Space, Nov. 2004, http://adsabs.harvard.edu/full/2005ESASP.563.479S.
[12] L.A. Dickinson, F. Jackson, A.L. Odgers, Erosive burning of polyurethane propellants in rocket engines, in: Proceedings of the 8th International Symposium on Combustion, Williams and Wilkins, Baltimore, MD, 1960, pp. 754–759.
[13] S. Gordon, B.J. McBride, Computer program for calculation of complex chemical equilibrium compositions and applications – II Users manual and program description, NASA RP-1311, 1996.